Environmental Science & Technology

pubs.acs.org/est

Article

Reaction of Substituted Phenols with Lignin Char: Dual Oxidative and Reductive Pathways Depending on Substituents and Conditions

Jing Li, Qingqing Li, Christian E. W. Steinberg, Qing Zhao, Bo Pan,* Joseph J. Pignatello,* and Baoshan Xing

Cite This: https://dx.doi.org/10.1021/acs.est.0c04991

Read Online

ACCESS | Metrics & More | Article Recommendations | Supporting Information

ABSTRACT: Biomass chars are known to be intrinsically redox-reactive toward some organic compounds, but the mechanisms are still unclear. To address this, a char made anoxically at 500 °C from dealkaline lignin was reacted either in the fresh state or after 180-day aging in air with *p*-nitrophenol (NO_2-P), *p*-hydroxybenzaldehyde (CHO-P), phenol (H-P), or *p*-methoxyphenol (MeO-P). The reactions were carried out under oxic or anoxic conditions. Degradation occurred in all cases. Both oxidation and reduction products were identified, with yields dependent on the presence or absence of air during reaction or storage. They included oligomers, amines, and ring-hydroxylated compounds, among others. Exposure to air suppressed sorption, annihilated reducing sites, and provided a source of reactive oxygen species that assisted degradation. Sorption suppression was due to the incorporation of hydrophilic groups by chemisorption of oxygen, and possibly blockage of sites by products. Fresh char has comparable electron-donating and accepting capacity, whereas there is a preponderance of electron-accepting over donating capacity in aged char. Under anoxic conditions, both oxidation and reduction occurred. Under oxic conditions or after aging in air, oxidation predominated, and linear free energy relationships were found between the rate constant and the Hammett or Brown substituent electronic parameter or the standard electrode potential of the phenol. The results demonstrate that chars possess heterogeneous redox activities depending on reaction pairs, reaction conditions, and aging.

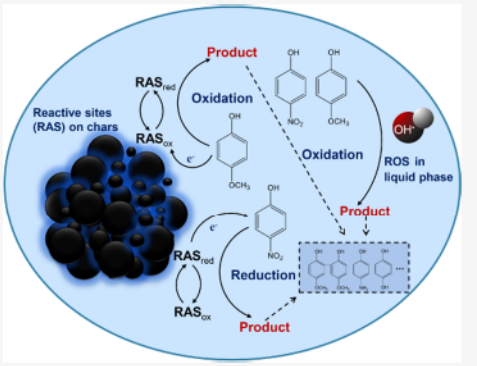

INTRODUCTION

Chars are the residues of pyrolysis or incomplete combustion of biomass. Fire-derived chars from wildfires and land management practices are widely dispersed in the environment.[1−5] Chars from pyrolysis of biomass wastes ("biochars") have attracted interest for use in agriculture and environmental management.[6,7] A principal focus of research on chars in these contexts is their strong ability to sorb organic compounds. As sorbents, chars distributed in the environment can impact the movement and bioavailability of chemicals in soil.[8−11] Moreover, sorptivity is central to the role of biochar and other carbonaceous materials employed in environmental remediation of soil and water.[6,12−17]

Researchers have become increasingly aware, however, that chars can have inherent chemical reactivity.[18−22] Chars can react with O_2 to produce reactive oxygen species (ROS), including $O_2^{\bullet-}$/ $HO_2^{\bullet}$, H_2O_2, and $HO^{\bullet}$,[23−25] at electron-rich defect sites[23] or persistent free radical (PFR) sites.[25,26] Graphite and activated carbon (AC) particles and fibers have long been known to cause oligomerization of phenols in the presence of air, leading to the often-observed "irreversible" sorption by these materials.[27] Initiation of phenol oligomerization has been attributed to ROS generated from O_2 reacting at defect, edge,[28,29] or basic functional group sites.[27,30−32] A free radical pathway involving ROS may be responsible for the degradation of organic compounds in biochar systems in the presence of added peroxides.[25,33,34] Chars are also capable of electrochemically donating or accepting electrons.[35−37] Electron-donating capacity (EDC) and electron-accepting capacity (EAC) of up to 7 and 0.4 mequiv/g, respectively, have been reported for pinewood-derived biochars.[37] Chars may act as electron shuttles between microbes and pollutants or between microbes and minerals due to EDC and EAC, provided electrical conductivity is sufficiently high.[38−40] Lastly, direct reactions between biochars and organic chemicals or metals have been reported.[21,22,41,42] To explain the reactions of chars with pollutants, researchers have implicated reactive sites (RAS), such as PFR,[21,22,33,43] defect,[28,29,44] or quinone/hydroquinone sites.[45−47]

We previously reported that a series of biochars[21] and model chars made from pure cellulose or lignin[22] are inherently

Received: July 26, 2020
Revised: October 17, 2020
Accepted: November 11, 2020

reactive toward *p*-nitrophenol (NO_2-P). The reaction occurs predominantly in the sorbed-state. Aging of the model chars for up to a month in moist air reduced but did not eliminate their reactivity.[22] The chars exposed to air chemisorb oxygen, liberating a portion as H_2O_2 when submerged in water while simultaneously degrading the evolved H_2O_2 to ROS. The results showed that direct reaction of NO_2-P with char predominates over H_2O_2-dependent reactions and that the majority of direct-reacting sites were non-radical in character. However, we could not confidently establish the reaction mechanism: both oxidation[21] and reduction[22] products of NO_2-P were identified, and the extent of NO_2-P degradation was correlated with the electron paramagnetic resonance (EPR) signal intensity of char particles in one study[21] but not the other.[22] We hypothesized that chars possess reducing or oxidizing capability, or both, depending on the char, aging period, and the redox properties of the compound.

To test this hypothesis, we selected a series of substituted phenols differing in electrode potential and substituent electronegativity to react with freshly-prepared chars under either oxic or anoxic conditions. Our previous study[22] indicated that aging fresh char in air annihilated sites reactive toward NO_2-P. To further investigate the influence of char aging on the sorption and degradation of phenols with different electronic properties under either oxic or anoxic conditions, we selected NO_2-P (the most electronegative phenol) and MeO-P (the most electropositive phenol) among the four phenols as models. The data collected on reactions conducted with these two phenols were enough to demonstrate the influence of the aging process. Lignin was chosen as the precursor material because it is substantially free of transition metals that can potentially mask the involvement of the carbon matrix and because overall, lignin char is much more reactive than cellulose char.[22]

EXPERIMENTAL SECTION

Materials. Dealkaline lignin was purchased from TCI. *p*-Nitrophenol (NO_2-P, >99.8%), *p*-hydroxybenzaldehyde (CHO-P, >99.0%), phenol (H-P, 99.5%), and *p*-methoxyphenol (MeO-P, 99.0%) were purchased from Sigma-Aldrich. Table S1 lists their relevant physicochemical properties. *N,O*-bis(trimethylsilyl)trifluoroacetamide (BSTFA, derivatization grade) used for gas chromatography/mass spectrometry (GC/MS) analysis was obtained from Sigma-Aldrich.

Preparation and Storage of Chars. Lignin char was prepared at 500 °C under N_2 using a method described in the previous study (details in the Supporting Information (SI)).[22] Portions of freshly-prepared chars were flame-sealed in brown glass ampules under vacuum and labeled fresh char; due to handling these portions had been exposed to air for about 0.5 h before evacuation. Other portions were stored in 40 mL brown glass vials open to room air for six months and labeled aged char. Lignin char prepared in our previous study in the same manner had a specific surface area of 231.4 m^2/g.[22] Another biochar prepared from rice straw at 1000 °C labeled RS10 was used for extractive recovery experiments. Table S2 lists the elemental content and pH of the chars.

Reaction Rates. Reactions were carried out in 8 mL glass vials sealed with a Teflon-lined septum screw cap. A solution of each phenol at an initial concentration of 1437 μmol/L was prepared in deoxygenated phosphate buffer (0.1 M, pH 3 ± 0.1) and stored in a glove box (O_2: 0 ppm; H_2: 1.5−2.0%) (COY-7000220A). Vials containing lignin char (90 mg) were mixed with 3 mL of a test phenol solution either in or outside the glove box to achieve either anoxic or oxic conditions, respectively. The pH of the mixtures was 6 ± 0.1. Under oxic conditions the O_2 content of the vials (~46.9 μmol) was more than 10 times greater than the initial phenol content (~4.3 μmol). The sealed vials were shaken on an orbital shaker in the dark at 20 °C. A replicate vial among those prepared was sacrificed at 0.5, 2, 4, 6, 8, 12, 16, and 24 h; then every day until 5 days; and finally every 5 days until the aqueous phase concentration leveled off or approached zero. The vials were centrifuged at 3000 rpm for 10 min, and the supernatant was filtered through a 0.45 μm syringe filter for HPLC analysis.

Sorbed phenol concentration was determined by hot-solvent extraction as in the previous study.[22] After removing as much supernatant as possible, the residue was weighed. Then acetonitrile (6 mL per vial) was added, and the vial was heated at 60 °C for 40 min. The extract was collected and filtered (0.45 μm) for analysis. This procedure was repeated several times until the test phenol concentration in the extract was below the HPLC detection limit. The extraction method was validated on RS10, an aged char that was presumed inert because it lacked EPR and DMPO-OH signals. After a 2 day equilibration period, the recovery of NO_2-P at 143.8 μmol/g initial concentration was 98.8 ± 0.6%.

The impact of O_2 on sorption and degradation was determined for fresh char with NO_2-P and MeO-P. To keep the mass ratio of phenol/char/water the same in every 16 mL vial, the char/liquid ratio was held constant at 300 mg/10 mL, 240 mg/8 mL, or 120 mg/4 mL, leaving a headspace volume of 6, 8, or 12 mL of air, respectively. The NO_2-P or MeO-P stock solution was delivered to the vial either in or out of the glove box to maintain either anoxic or oxic conditions, respectively. After a 2 day reaction, the supernatant phase and acetonitrile extracts of the char particles were analyzed for the test phenol concentration.

Analytical Methods. The phenols were quantified in the supernatant phase and acetonitrile extracts by elution through a C18-silica column (3.0 mm × 150 mm, 2.7 μm, Brownlee, SPP) with 50:50 (v/v) acetonitrile−deionized water at 1.0 mL/min, and the analyte was detected with a diode array detector at 318 (NO_2-P), 280 (CHO-P), 272 (H-P), or 290 (MeO-P) nm (Shimadzu Prominence high-performance liquid chromatography system). To identify products, acetonitrile extracts of char particles and freeze-dried supernatant samples were first derivatized with BSTFA and then analyzed by GC/MS (Shimazu, QP2010) (details in the SI). PFRs and $HO^{\bullet}$ were determined by electron paramagnetic resonance (EPR) spectroscopy on a Bruker A300-6/1 (details in the SI).

The EAC and EDC of the chars were determined by the method of Xin et al. (eqs 1 and 2, respectively).[36]

$$\text{char} + \text{Ti(III)} \rightarrow \text{char}_{\text{red}} + \text{Ti(IV)} \quad (1)$$

$$\text{char} + [\text{Fe(III)(CN)}_6]^{3-} \rightarrow \text{char}_{\text{ox}} + [\text{Fe(II)(CN)}_6]^{4-} \quad (2)$$

The measurements and calculations are described in the SI (Figures S1 and S2).

The functional groups of the chars were characterized using Fourier transform infrared spectrometry (Varian 640-IR).

C 1s X-ray photoelectron spectra (XPS) of chars were obtained on a PHI 5000 VersaProbe-II spectrometer (ULVAC-PHI, Japan).

https://dx.doi.org/10.1021/acs.est.0c04991
Environ. Sci. Technol. XXXX, XXX, XXX−XXX

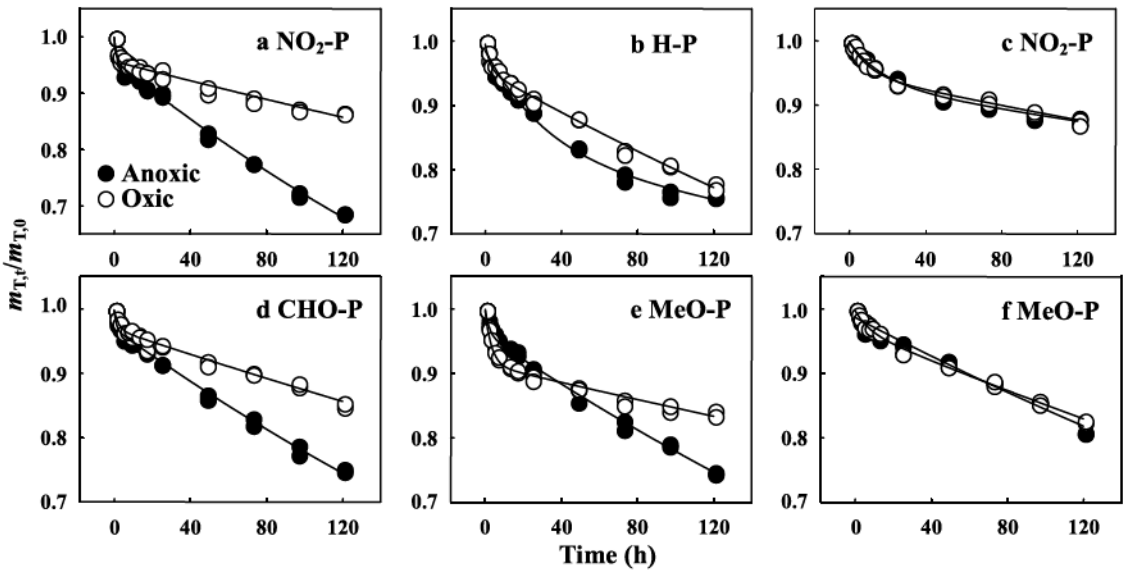

Figure 1. Degradation of phenols (time decay of total mass in the vessel) in the presence of fresh char (a, b, d, e) and aged char (c, f). Reaction conditions: anoxic (●) and oxic (○). Curves represent the fit to the dual-stage first-order rate law.

RESULTS

Degradation Kinetics. Experiments were conducted with fresh char for all four phenols and with aged char for NO_2-P and MeO-P, which, respectively, have the most electronegative and electropositive substituent. Reaction of the test phenol was observed in all cases. Control experiments indicate that H_2 in the headspace from the glove box did not participate in reactions: (a) NO_2-P was still reduced by fresh char in anoxic reactions without H_2, and (b) no NO_2-P reduction products were found after reaction with aged char in anoxic reactions with H_2. Declines in the aqueous phase concentration (C_{aq}) during 120 h (aged char) or 480 h (fresh char) periods are plotted in Figure S3. These curves show that removal is rapid at first and then tapers off. The aqueous C_{aq} of all compounds for fresh char under anoxic conditions reached zero by 360 h. The decline in C_{aq} was incomplete in other cases. Interpretation of these curves was made difficult by the fact that sorption/desorption and reaction were occurring simultaneously. It is thus more informative to monitor total mass in the vessel, m_T, which is the sum of sorbed mass (m_s) and dissolved mass (m_{aq}), during the reaction. Independent measurements of m_s and m_{aq} were obtained at each time-point over the first 120 h. Figure 1 shows that the loss of m_T generally proceeds in a faster stage lasting a few hours, followed by a slower stage.

The decay curves of Figure 1 were fitted to a dual-stage first-order rate law given in eq 3

$$\frac{m_{T,t}}{m_{T,0}} = F_{fast}\, e^{-k_{fast}t} + F_{slow}\, e^{-k_{slow}t} \quad (3)$$

where F is the mass fraction ($F_{fast} + F_{slow} = 1$) and k is the rate constant corresponding to the fast-reacting and slow-reacting stage. Equation 3 assumes that sites initiating the reaction are not depleted. The fitting parameters appear in Table S3. Table S3 shows that the fast stage generally comprises a small fraction of the observed degradation (<17% in all cases; <9% in all but one case) and thus may correspond to the sites that are more reactive or more available or both.

Rate constants assuming that the phenols react predominantly in the sorbed-state were also estimated. In that case, the elementary rate law can be expressed by

$$-\frac{dm_T}{dt} = k_s(\mathrm{RAS}) \times m_s \quad (4)$$

where k_s(RAS) is a rate constant (h^{-1}) that is a function of the (time-dependent) quantity of reactive sites (RAS) on the char. Equation 4 could not be solved analytically because the functional relationship between m_T and m_s, as well as how the quantity of RAS depends on time, are unknown. The variation of k_s(RAS) with time can be calculated numerically, however (details in SI section I). Values at short times had high uncertainties reflecting the low percent conversion. Values at times greater than 10 h (>four half-lives of reaction in the fast stage) were relatively stable. Thus the average value after 10 h was taken to represent the sorbed-state rate constant for the slow stage, $k_{s,\,slow}$ (Table S3).

The results in Figure 1 and Table S3 show that degradation by fresh char is more rapid and extensive when the reaction is carried out under anoxic than oxic conditions, but that degradation rate and extent by aged char are almost identical under the two conditions. In addition, for the reaction of two compounds (NO_2-P and MeO-P) with aged char, the results indicate that aging suppresses the rate and extent of degradation under anoxic conditions, but aging has little effect under oxic conditions. The exception is that the initial fast stage of MeO-P oxic degradation is substantially reduced by aging. All of these trends originate from the multiple and interconnected roles of O_2, which will be discussed in the following sections.

Linear Free Energy Relationships (LFERs). LFERs were tested between k_{fast} or k_{slow}, and certain electronic free energy parameters listed in Table S1. The Hammett σ_p and Brown σ_p^+ constants reflect the ability of the substituent to withdraw electron density affecting reactivity at the ring C or −OH group. The σ_p incorporates resonance and inductive effects of the substituent, whereas σ_p^+ emphasizes resonance effects. Although they were derived for two-electron (acid-base, nucleophilic) reactions, they have also been applied to

https://dx.doi.org/10.1021/acs.est.0c04991
Environ. Sci. Technol. XXXX, XXX, XXX−XXX

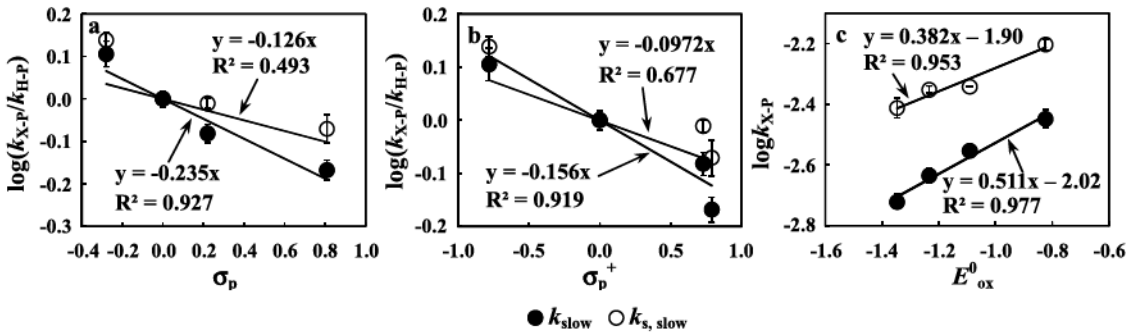

Figure 2. Linear free energy relationships between k_{slow} (●) or $k_{s,\,slow}$ (○) and electronic free energy parameters, including Hammett σ_p (a), Brown σ_p^+ (b), and E_{ox}^0 (c), for the reaction of fresh char under oxic conditions.

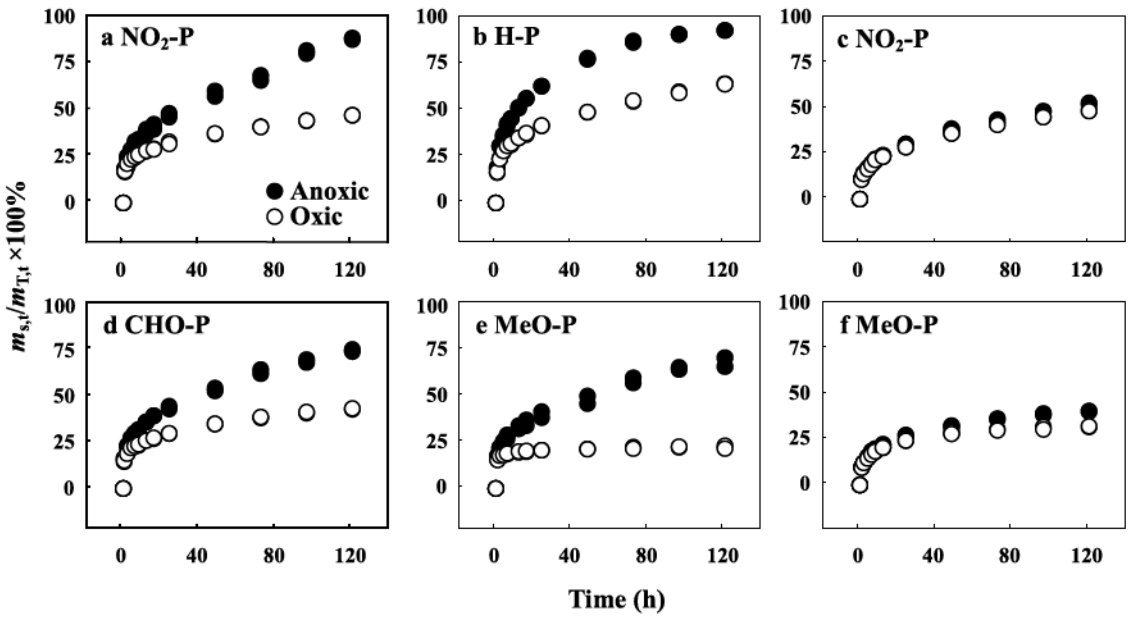

Figure 3. Sorbed test phenol as a percentage of all unreacted test phenol during the reaction under anoxic (●) or oxic (○) conditions. *p*-nitrophenol (NO_2-P), *p*-hydroxybenzaldehyde (CHO-P), phenol (H-P), and *p*-methoxyphenol (MeO-P). Reaction system: fresh char (a, b, d, e), aged char (c, f).

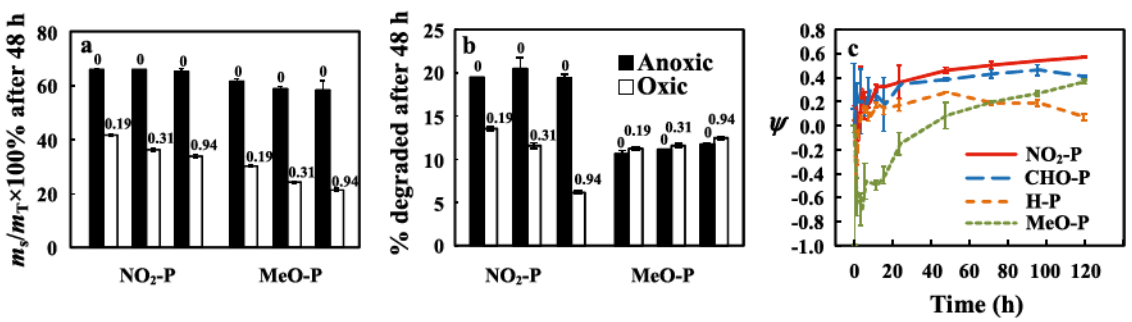

Figure 4. Impact of the oxygen content on sorption (a) and degradation (b) of NO_2-P and MeO-P by fresh char under anoxic (■) or oxic (□) conditions after a 48 h reaction period. Number above each black or white bar is the initial headspace O_2 concentration in mmol O_2/g char. The oxygen inhibitory effect ψ (c) on the degradation of the phenols with reaction time for fresh char.

photocatalytic decomposition[48] and electrochemical reaction.[49] The corresponding LFER is given by

$$\log \frac{k_{X-P}}{k_{H-P}} = \rho \times (\sigma_p \text{ or } \sigma_p^+) \quad (5)$$

where X is the substituent and ρ is a constant reflecting sensitivity to substituent electronic effects.

The standard electrode potential E_{ox}^0 for the half-reaction, Ar−OH → Ar−O$^\bullet$ + e$^-$ + H$^+$, reflects the thermodynamic ability of phenol to donate an electron to an oxidant site or species. The appropriate LFER with E_{ox}^0 is given by

$$\log k_{X-P} = \alpha E_{ox}^0 + \beta \quad (6)$$

where α and β are regression coefficients. The ability to accept an electron from a reducing site or species is difficult to test

https://dx.doi.org/10.1021/acs.est.0c04991
Environ. Sci. Technol. XXXX, XXX, XXX−XXX

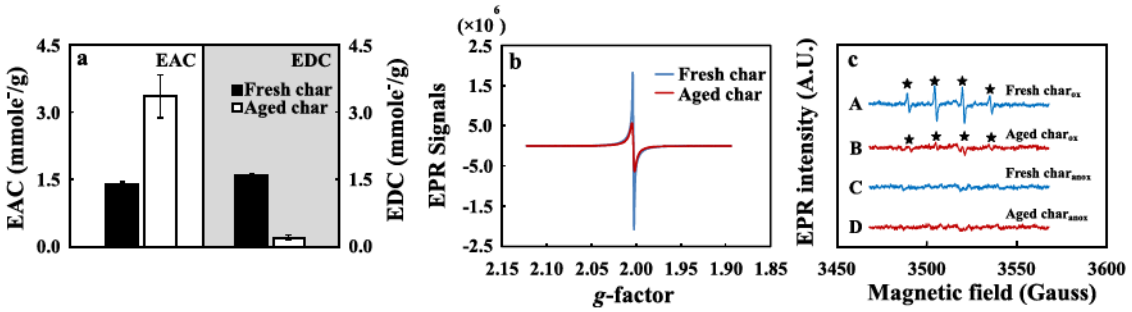

Figure 5. (a) Electron-accepting capacity (EAC, white region) and electron-donating capacity (EDC, gray region) of fresh char (■) and aged char (□). (b) EPR signals of fresh char (blue line) and aged char (red line). (c) EPR signals of DMPO-OH adducts (★) in fresh char (blue line) and aged char (red line) reaction systems under oxic (A, B) or anoxic conditions (C, D).

using an analogous LFER because E_{red}^0 (Ar−OH/Ar−OH$^{-\bullet}$) values are unavailable.

Correlations based on eqs 5 and 6 for the slow stage under oxic conditions are strong (Figure 2): log k_{slow} decreases with substituent electron-withdrawing ability (σ_p or σ_p^+), or increases with E_{ox}^0, as expected for an oxidative pathway predominating under oxic conditions. Assigning all degradation to molecules in the sorbed-state ($k_{s,slow}$) gives similar trends as k_{slow}, although the correlations are not as good (Figure 2).

By contrast, LFERs for k_{fast} under both oxic and anoxic conditions or for k_{slow} under anoxic conditions are generally poor (Figure S6). The poor correlations for k_{fast} may be simply a consequence of the high inaccuracy of data during the fast stage due to low percent conversion. The poor correlations for k_{slow} under anoxic conditions may be attributed to the occurrence of both oxidation and reduction reactions taking place, as we propose later based on the products and other evidence.

Influence of Oxygen. Oxygen is found to play several interconnected roles. First, its chemisorption suppresses the sorption of the test phenols. Figure 3 plots sorbed mass (m_s, determined by solvent extraction) as a percentage of remaining (unreacted) mass of the phenol (m_T) during degradation. The ratio $m_{s,t}/m_{T,t}$ reflects the partitioning of the phenol between water and char at specific times during degradation. Exposure of the char to air, either by aging in air or including air in the headspace during degradation, generally inhibits sorption of the test phenols (Figure 3). The greatest effect appears to be on MeO-P sorption. Figure 4a,b show the results of O_2 gradient experiments on fresh char for the two phenols with the most and least electronegative substituent (NO_2-P and MeO-P). The volume of air in the vial headspace was adjusted to achieve 0, 0.19, 0.31, or 0.94 mmol O_2/g char. Figure 4a shows that, relative to the anoxic control (black bars), sorption is suppressed in proportion to headspace O_2 content for both compounds.

One likely explanation for the suppressive effect of O_2 on sorption is that oxygen chemisorption increases the hydrophilic character of the char surface. The O content is higher and the C content is lower in aged char compared to fresh char (Table S2). The Fourier transform infrared (FT-IR) spectra indicate oxygenation of the char surface after aging (Figure S7). The C 1s XPS spectra show an increase in the abundance of hydroxyl and carboxyl groups after aging in air, whereas no change was observed in the absence of air (Figure S8). Water molecules cluster around polar functional groups in carbonaceous solids by hydrogen bonding, thereby reducing the surface area and pore volume available for the sorption of organic compounds.[50−53] Molecular simulations of porous carbons show crowding out of methane by water as sites on pore walls become populated with polar groups.[54,55] In a study of carbon spheres, removal of polar groups favored H-P sorption.[56]

Oxygen plays a second role by scavenging reducing sites and PFR sites that are potentially redox-reactive toward the test phenols. The molecular sizes of O_2, $O_2^{\bullet-}$, and H_2O_2 are smaller than those of the phenols, so they have better access to reducing sites and consequently can compete with the phenol for electrons. Figure 4b shows that, relative to the anoxic control, the percent degraded declines in proportion to the headspace O_2 content for NO_2-P, but is unaffected by O_2 (even slightly enhanced) for MeO-P. Given that O_2 inhibits sorption of both compounds (Figures 3 and 4a), Figure 4b suggests that O_2 has opposing effects: it reduces the sorbed concentration, which limits the reaction with active sites, while at the same time altering the redox function of the char. Redox function is altered by the annihilation of reducing sites. Oxygen suppression of NO_2-P reduction by chemical reagents is well known.[57−59] Annihilation of reactive sites of lignin char by O_2 was shown in our previous study.[22] Such annihilation is further demonstrated here by the electrochemical analysis shown in Figure 5a, which reveals that fresh char has both EDC and EAC in comparable amounts, whereas aging causes a decrease in the EDC commensurate with an increase in the EAC. Figure 5b shows that aging causes ~75% decline in the PFR concentration as measured by the EPR signal intensity. The previous study[22] showed about a 60% (lignin char) or 20% (cellulose char) decline in the PFR concentration after the first few hours of aging in moist air, followed by a leveling off over the subsequent 30 days.

Oxygen plays a third role by reacting with reducing sites to form ROS that can attack the phenol. Generation of ROS is verified by the appearance of the DMPO-OH adduct in solution with both fresh and (to a lesser extent) aged char under oxic conditions, but no DMPO-OH adduct under anoxic conditions (Figure 5c). The results of the oxygen gradient experiments in Figure 4 can be interpreted to mean that, while degradation is inhibited by the sorption suppression generally, degradation of the most electronegative phenol (NO_2-P) is further inhibited by O_2 scavenging of reducing sites, whereas degradation of the most electropositive phenol (MeO-P) is counterbalanced by creation of EAC sites or generation of ROS from O_2. Finally, it is noted after the comparison of fresh char and aged char in Figures 1, 3, and S3 that aging of chars in air diminishes the net impact of O_2 on sorption and degradation.

https://dx.doi.org/10.1021/acs.est.0c04991
Environ. Sci. Technol. XXXX, XXX, XXX−XXX

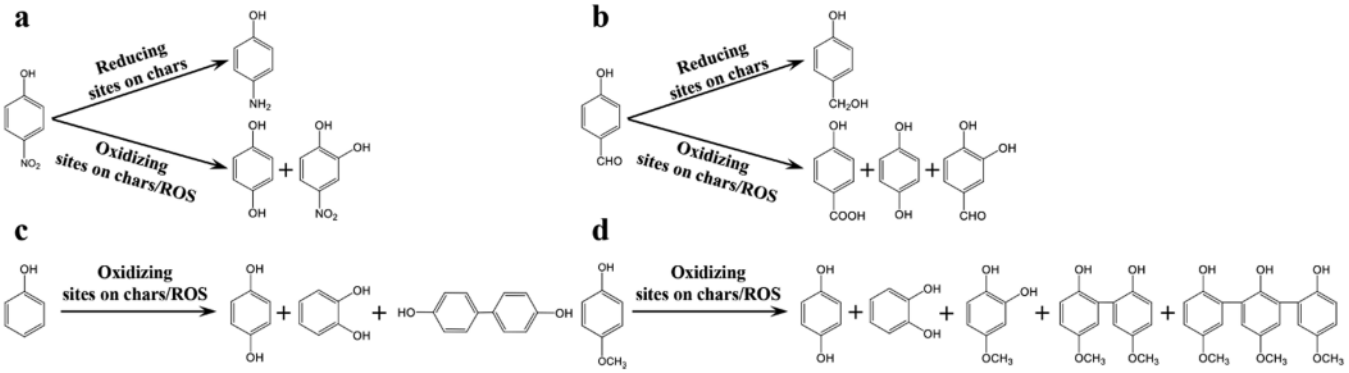

Figure 6. Initial degradation products of phenols: (a) *p*-nitrophenol (NO_2-P), (b) *p*-hydroxybenzaldehyde (CHO-P), (c) phenol (H-P), and (d) *p*-methoxyphenol (MeO-P).

To put the overall impact of oxygen on the degradation of the phenols by fresh char into a more quantitative perspective, an oxygen inhibitory effect (ψ) was defined by using data taken from Figure 1.

$$\psi = (\text{fraction degraded}_{\text{anox}} - \text{fraction degraded}_{\text{ox}}) / \text{fraction degraded}_{\text{anox}} \quad (7)$$

The values of ψ for fresh char are compared in Figure 4c over a 120 h reaction period. Data before ~ 5 h are erratic due to large errors in the measurement. After that time, several key features of Figure 4c are identified. (1) Between ~5 and ~70 h, O_2 inhibits degradation in the same order of the electron-withdrawing capability of the substituent: NO_2-P > CHO-P > H-P ≫ MeO-P. This is consistent with the role of O_2 as a scavenger of reducing sites such that O_2 becomes less competitive for reducing sites along this series of phenols. The general upward trend in ψ with substituent electronegativity over this period for all but H-P most likely reflects the decreasing role of reducing sites in degradation. Why the H-P curve inflects is unclear at this time. (2) Oxygen has an accelerating effect on MeO-P degradation up to ~50 h, and an inhibitory effect thereafter. The curve for MeO-P crosses over the curve for H-P at ~65 h, at which point MeO-P falls out of order among the phenols based on substituent electronic effects. The differing effect of oxygen on the phenols can be explained by the participation of HO$^\bullet$ under oxic conditions and by the effects of oxygen chemisorption on test phenol sorption. The generation of HO$^\bullet$ falls off rapidly after exposure of fresh char to air.[22] The falloff contributes to the increasing value of ψ with reaction time except in the case of H-P. Having the most electropositive substituent, MeO-P is the most reactive of the test phenols toward HO$^\bullet$ [$k_{\text{MeO-P}} = 26 \times 10^9$, $k_{\text{CHO-P}} = 12.1 \times 10^9$, $k_{\text{H-P}} = (6.6–11.8) \times 10^9$, $k_{\text{NO2-P}} = 3.8 \times 10^9$ M^{-1} s^{-1}].[60,61] This fact explains the stimulatory effect of O_2 on MeO-P degradation before ~50 h (i.e., the negative value of ψ). It also explains the greater positive slope of the ψ curve for MeO-P than for other phenols, since the decline in HO$^\bullet$ would have a larger negative impact on MeO-P degradation under oxic conditions compared to the other phenols. A second fact explains the deviation of MeO-P from the abovementioned order in phenol reactivity at longer times: Figures 3 and 4a both show that MeO-P sorption is the most sensitive to oxygen chemisorption among phenols. The cause of greater sorption inhibition of MeO-P requires further investigation. It is possible that reaction products block oxidative sites more so for MeO-P than for the other phenols. Dimers were identified for both H-P and MeO-P, and a trimer was found for MeO-P (Figures S9, S10, and S11). Xie et al. detected dimer, trimer, and even tetramer products of MeO-P when it reacted with reduced graphene in the presence of oxygen.[29] Grant and King proposed that oxidative-coupling products could block sites and/or micropores of AC. Among the test phenols in their study, which included all four of the test compounds here, MeO-P was the most reactive in oxidative-coupling reactions with AC under oxic conditions and showed the greatest "irreversible" sorption.[62]

Degradation Products. Different degradation products were detected in anoxic and oxic systems with fresh char and aged char. The major initial products are shown in Figure 6. The chromatograms are shown in Figure S9 and the mass spectra of the trimethylsilyl derivatives are shown in Figures S10–S14. All products appeared only in the presence of a phenol except benzene-1,2-diol (catechol), which appeared in control samples, usually at a lower concentration (Figure S15). It is known that catechol is produced in significant yield in the pyrolysis of alkali lignin at 500 °C.[63]

Products from NO_2-P included benzene-1,4-diol (hydroquinone), 4-aminophenol, and 2-hydroxy-4-nitrophenol. Products from CHO-P included hydroquinone, 4-hydroxybenzyl alcohol, 2,4-dihydroxybenzaldehyde, and 4-hydroxybenzoic acid. Products from H-P included catechol, hydroquinone, and two dimers. Products from MeO-P included catechol, hydroquinone, 2-hydroxy-4-methoxyphenol, a dimer, and a trimer.

Reduction products (*p*-aminophenol from NO_2-P and *p*-hydroxybenzyl alcohol from CHO-P) were detected only for phenols with strongly electronegative substituents, only in anoxic systems, and only for fresh char. By contrast, oxidation products of all four compounds were detected under both anoxic and oxic conditions and at much lower concentrations in aged than in fresh char. Dimers, trimers (only for MeO-P), or their hydroxylated products were detected only for H-P and MeO-P. The molecular weights of these oligomers followed a pattern of $nM - 2(n - 1)$, where n is an integer, and are likely formed via radical–radical coupling reactions.[29,64,65] The oligomers appeared under both anoxic and oxic conditions, for both fresh and aged chars, and predominantly in solid-phase extracts.

DISCUSSION

The overall mechanism based on the results here and our previous reports[21,22] is shown schematically in the abstract

https://dx.doi.org/10.1021/acs.est.0c04991
Environ. Sci. Technol. XXXX, XXX, XXX–XXX

graphic. The phenol is oxidized or reduced by RAS on the char or is oxidized by ROS present in pores or bulk solution that originate from the reaction of O_2 with RAS. Issues that have been addressed in this study include whether and under what circumstances reduction or oxidation predominates, whether reaction occurs predominantly with RAS or in solution, the influence of molecular oxygen, and the nature of RAS.

The phenols react under all tested conditions. Generally, the reaction is faster under anoxic than oxic conditions for fresh char, but the rates are about equal for aged char. Reduction products appear only under anoxic conditions and only with fresh char, while oxidation products appear under both anoxic and oxic conditions for both fresh and aged chars. It is possible that reduction products formed under oxic conditions were subsequently oxidized by ROS,[59] but we found no evidence for this. The reaction rate constant for fresh char under oxic conditions correlates strongly with substituent electronic parameters or electrode potential of the phenol, consistent with oxidation predominating under oxic conditions. By contrast, under anoxic conditions, correlations between the rate constant and the substituent electronic parameters are poor, reflecting the fact that both oxidation and reduction occur under anoxic conditions. Electrochemical experiments show that EDC and EAC were present in similar amounts in fresh char, whereas EAC was present in large excess relative to EDC in aged char (Figure 5a). Thus, air reduces EDC and increases EAC. This may explain why fresh char under anoxic conditions acts as both an oxidant and reductant, while aged char or fresh char under oxic conditions acts predominantly as an oxidant toward phenols. We thus propose that the reactive sites on char are diverse in their redox potential, exhibiting oxidizing and reducing capability depending on the degree of aging of the chars and the redox properties of the phenols.

Our previous studies showed that degradation of NO_2-P under oxic conditions correlates with the sorbed concentration.[21,22] The present study reinforces this conclusion by finding that under oxic conditions, the rate constants of sorbed-state phenol ($k_{s,slow}$) correlate in an expected manner with substituent electronic parameters and redox potential of the phenol. Nevertheless, under oxic conditions, oxidation may occur with ROS as well. Hydroxyl radicals under oxic conditions have been identified by EPR spectroscopy in many systems,[21,22,25] as well as in the present study (Figure 5c). They presumably are generated by the reaction of H_2O_2 within char pores. Detection of $HO^{\bullet}$ does not necessarily mean it plays a major role in degradation. Due to their high and indiscriminate reactivity, most $HO^{\bullet}$ likely react with pore walls within a short diffusion distance. Those that survive annihilation can react with dissolved molecules in water-filled meso- or macropores or in bulk solution. The previous study[22] found that ROS oxidation of NO_2-P played a minor role (probably <30%) in its degradation. However, it is likely that ROS plays a more important role in oxic degradation of phenols having more electropositive substituents, such as MeO-P. Clearly, oxidation of the phenols by chars in the absence of O_2 must have occurred with the direct-reacting sites since no O_2-derived ROS would be available.

In contrast with oxidation, reduction of phenols under anoxic conditions, whether with fresh or aged char, must have occurred almost exclusively on particles since no O_2 was present to generate ROS, and the liquid phase probably lacked dissolved electron carrier species that could lead to phenol reduction in solution. We thus conclude that the degradation of phenols under anoxic conditions is determined mainly by the abundance and accessibility of RAS on the char.

The present study does not shed any light on the identity(ies) of the RAS. It has previously been proposed that PFRs are derived from hydroquinone/quinone-like structures on the char and that they function as a one-electron oxidant or reductant. We concluded previously[22] that PFR plays a minor role in the reaction of NO_2-P with lignin and cellulose chars. The quantitative role of PFR may depend on the phenol, the electrode potential of the phenol, and conditions. The PFR concentration is diminished considerably but not eliminated by storage in air. In principle, PFR can react with sorbed molecules as a one-electron oxidant or reductant. The PFR can subsequently be regenerated by transferring its acquired electron to an oxidant such as O_2, if present, or by accepting an electron from a suitable reductant, which would have to be added if it is not naturally present. Further work is needed to identify these reactive moieties.

Oxygen destroys reducing sites and suppresses sorption, both of which can lower the reaction rate. Destruction of reducing sites is evident by the effects of O_2 on the product distribution (Figures 6 and S9) and reaction rate (Figures 1 and 4b), and by the decline in EDC with aging (Figure 5a). Sorption inhibition in oxygen-exposed situations is clear from the data in Figures 3 and 4a and is most likely due to the formation of a more hydrophilic surface.

This study is the first to provide insight into the relationship between the redox properties of substituted phenols and their degradation by chars. It also defines the impact of oxygen on the reactivity of the char-containing system to different phenols, including its negative effect on sorption. In addition, it explains why both oxidation and reduction of NO_2-P by chars take place.[21,22] In many other studies, reduction of nitroaromatic compounds with carbonaceous materials required the addition of an external reductant (e.g., nZVI, borohydride, H_2S, and Na_2S). In contrast, the present study indicates that fresh char itself can act as a reductant toward some easily-reduced compounds, such as NO_2-P and CHO-P. In addition, we observed that chars generally possess oxidizing ability toward a wider variety of compounds. Particularly, fresh char can induce ROS reactions easily in the presence of oxygen, avoiding the need for an extra oxidant (e.g., H_2O_2) as for other carbonaceous materials. Therefore, the fate and risk of organic chemicals, especially phenolic compounds, should be carefully investigated in the black carbon-rich environments. Our study also illustrates that chars have potential remediation functions for polluted soil or water. During application, the abundance and properties of redox sites on char can be manipulated through modification of reaction conditions according to the redox properties of the target compounds.

■ ASSOCIATED CONTENT

Supporting Information

The Supporting Information is available free of charge at https://pubs.acs.org/doi/10.1021/acs.est.0c04991.

Reduction of chars by Ti(III) citrate; oxidation of chars by ferricyanide as a function of time; removal of phenols from the aqueous phase; k_s(RAS) of phenols with time; linear free energy relationships; FT-IR spectra; XPS spectra; initial degradation products; some physicochemical properties of the four test phenols; elemental composition (%) and atomic ratios; and parameters of

https://dx.doi.org/10.1021/acs.est.0c04991
Environ. Sci. Technol. XXXX, XXX, XXX−XXX

dual-stage first-order rate law and sorbed-state rate constants for phenols (PDF)

AUTHOR INFORMATION

Corresponding Authors

Bo Pan − *Yunnan Provincial Key Laboratory of Soil Carbon Sequestration and Pollution Control, Faculty of Environmental Science & Engineering, Kunming University of Science & Technology, Kunming 650500, Yunnan, China;* orcid.org/0000-0003-3680-1451; Phone: 86-871-65102829; Email: panbocai@gmail.com

Joseph J. Pignatello − *Department of Environmental Sciences, The Connecticut Agricultural Experiment Station, New Haven, Connecticut 06504, United States;* orcid.org/0000-0002-2772-5250; Phone: 203-974-8518; Email: joseph.pignatello@ct.gov

Authors

Jing Li − *Yunnan Provincial Key Laboratory of Soil Carbon Sequestration and Pollution Control, Faculty of Environmental Science & Engineering, Kunming University of Science & Technology, Kunming 650500, Yunnan, China; Stockbridge School of Agriculture, University of Massachusetts, Amherst, Massachusetts 01003, United States;* orcid.org/0000-0003-4297-384X

Qingqing Li − *Stockbridge School of Agriculture, University of Massachusetts, Amherst, Massachusetts 01003, United States*

Christian E. W. Steinberg − *Yunnan Provincial Key Laboratory of Soil Carbon Sequestration and Pollution Control, Faculty of Environmental Science & Engineering, Kunming University of Science & Technology, Kunming 650500, Yunnan, China; Faculty of Life Sciences, Laboratory of Freshwater & Stress Ecology, Humboldt-Universität zu Berlin, 12437 Berlin, Germany*

Qing Zhao − *Institute of Applied Ecology, Chinese Academy of Sciences, Shenyang 110016, China;* orcid.org/0000-0003-2250-5571

Baoshan Xing − *Stockbridge School of Agriculture, University of Massachusetts, Amherst, Massachusetts 01003, United States;* orcid.org/0000-0003-2028-1295

Complete contact information is available at: https://pubs.acs.org/10.1021/acs.est.0c04991

Notes

The authors declare no competing financial interest.

ACKNOWLEDGMENTS

This work was supported by grants from the National Natural Scientific Foundation of China (41725016), the National Science Foundation of the U.S. (CHE 1709532), and the USDA Hatch Program (MAS 00549). The authors would also like to thank the China Scholarship Council for financial support as a Ph.D. student scholarship to J.L. at the University of Massachusetts, Amherst.

REFERENCES

(1) Lighty, J. S.; Veranth, J. M.; Sarofim, A. F. Combustion aerosols: factors governing their size and composition and implications to human health. *J. Air Waste Manage. Assoc.* **2000**, *50*, 1565−1618.

(2) Masiello, C. A. New directions in black carbon organic geochemistry. *Mar. Chem.* **2004**, *92*, 201−213.

(3) Masiello, C. A.; Druffel, E. R. M. Black carbon in deep-Sea sediments. *Science* **1998**, *280*, 1911−1913.

(4) Middelburg, J. J.; Nieuwenhuize, J.; Breugel, P. V. Black carbon in marine sediment. *Mar. Chem.* **1999**, *65*, 245−252.

(5) Schmidt, M. W. I.; Noack, A. G. Black carbon in soils and sediments: Analysis, distribution, implications, and current challenges. *Global Biogeochem. Cycles* **2000**, *14*, 777−793.

(6) Lehmann, J.; Joseph, S. *Biochar for Environmental Management: Science, Technology and Implementation*; Routledge: New York, NY, 2015.

(7) Jeffery, S.; Verheijen, F. G. A.; van der Velde, M.; Bastos, A. C. A quantitative review of the effects of biochar application to soils on crop productivity using meta-analysis. *Agric., Ecosyst. Environ.* **2011**, *144*, 175−187.

(8) Sander, M.; Pignatello, J. J. Characterization of Charcoal Adsorption sites for Aromatic Compounds: Insights Dran from Single-Solute and Bi-Solute Competitive Experiments. *Environ. Sci. Technol.* **2005**, *39*, 1606−1615.

(9) Cornelissen, G.; Gustafsson, O.; Bucheli, T. D.; Jonker, M. T. O.; Koelmans, A. A.; van Noort, P. C. M. Extensive sorption of organic compounds to black carbon, coal, and kerogen in sediments and soils: Mechanisms and consequences for distribution, bioaccumulation, and biodegradation. *Environ. Sci. Technol.* **2005**, *39*, 6881−6895.

(10) Cornelissen, G.; Haftka, J.; Parsons, J.; Gustafsson, O. Sorption to black carbon of organic compounds with varying polarity and planarity. *Environ. Sci. Technol.* **2005**, *39*, 3688−3694.

(11) Lian, F.; Xing, B. Black Carbon (Biochar) In Water/Soil Environments: Molecular Structure, Sorption, Stability, and Potential Risk. *Environ. Sci. Technol.* **2017**, *51*, 13517−13532.

(12) Chen, Q.; Zheng, J.; Zheng, L.; Dang, Z.; Zhang, L. Classical theory and electron-scale view of exceptional Cd(II) adsorption onto mesoporous cellulose biochar via experimental analysis coupled with DFT calculations. *Chem. Eng. J.* **2018**, *350*, 1000−1009.

(13) Keiluweit, M.; Nico, P. S.; Johnson, M. G.; Kleber, M. Dynamic molecular structure of plant biomass-derived black carbon (biochar). *Environ. Sci. Technol.* **2010**, *44*, 1247−1253.

(14) Mohan, D.; Sarswat, A.; Ok, Y. S.; Pittman Jr, C. U. Organic and inorganic contaminants removal from water with biochar, a renewable, low cost and sustainable adsorbent−a critical review. *Bioresour. Technol.* **2014**, *160*, 191−202.

(15) Tan, X.; Liu, Y.; Zeng, G.; Wang, X.; Hu, X.; Gu, Y.; Yang, Z. Application of biochar for the removal of pollutants from aqueous solutions. *Chemosphere* **2015**, *125*, 70−85.

(16) Teixidó, M.; Hurtado, C.; Pignatello, J. J.; Beltran, J. L.; Granados, M.; Peccia, J. Predicting contaminant adsorption in black carbon (biochar)-amended soil for the veterinary antimicrobial sulfamethazine. *Environ. Sci. Technol.* **2013**, *47*, 6197−6205.

(17) Xiao, F.; Bedane, A. H.; Zhao, J. X.; Mann, M. D.; Pignatello, J. J. Thermal air oxidation changes surface and adsorptive properties of black carbon (char/biochar). *Sci. Total Environ.* **2018**, *618*, 276−283.

(18) Chacón, F. J.; Cayuela, M. L.; Roig, A.; Sánchez-Monedero, M. A. Understanding, measuring and tuning the electrochemical properties of biochar for environmental applications. *Rev. Environ. Sci. Bio/Technol.* **2017**, *16*, 695−715.

(19) Pignatello, J. J.; Mitch, W. A.; Xu, W. Activity and Reactivity of Pyrogenic Carbonaceous Matter toward Organic Compounds. *Environ. Sci. Technol.* **2017**, *51*, 8893−8908.

(20) Xu, W.; Pignatello, J. J.; Mitch, W. A. Reduction of nitroaromatics sorbed to black carbon by direct reaction with sorbed sulfides. *Environ. Sci. Technol.* **2015**, *49*, 3419−3426.

(21) Yang, J.; Pan, B.; Li, H.; Liao, S.; Zhang, D.; Wu, M.; Xing, B. Degradation of *p*-Nitrophenol on Biochars: Role of Persistent Free Radicals. *Environ. Sci. Technol.* **2016**, *50*, 694−700.

(22) Yang, J.; Pignatello, J. J.; Pan, B.; Xing, B. Degradation of *p*-Nitrophenol by Lignin and Cellulose Chars: H_2O_2-Mediated Reaction and Direct Reaction with the Char. *Environ. Sci. Technol.* **2017**, *51*, 8972−8980.

(23) Rey, A.; Zazo, J. A.; Casas, J. A.; Bahamonde, A.; Rodriguez, J. J. Influence of the structural and surface characteristics of activated

https://dx.doi.org/10.1021/acs.est.0c04991
Environ. Sci. Technol. XXXX, XXX, XXX−XXX

carbon on the catalytic decomposition of hydrogen peroxide. *Appl. Catal., A* **2011**, *402*, 146−155.
(24) Kimura, M.; Miyamoto, I. Discovery of the activated-carbon radical AC^+ and the novel oxidation-reactions comprising the AC/AC^+ cycle as a catalyst in an aqueous-solution. *Bull. Chem. Soc. Jpn.* **1994**, *67*, 2357−2360.
(25) Fang, G.; Zhu, C.; Dionysiou, D. D.; Gao, J.; Zhou, D. Mechanism of hydroxyl radical generation from biochar suspensions: Implications to diethyl phthalate degradation. *Bioresour. Technol.* **2015**, *176*, 210−217.
(26) Fang, G.; Liu, C.; Gao, J.; Zhou, D. New insights into the mechanism of the catalytic decomposition of hydrogen peroxide by activated carbon: implications for degradation of diethyl phthalate. *Ind. Eng. Chem. Res.* **2014**, *53*, 19925−19933.
(27) Dąbrowski, A.; Podkoscielny, P.; Hubicki, Z.; Barczak, M. Adsorption of phenolic compounds by activated carbon−a critical review. *Chemosphere* **2005**, *58*, 1049−1070.
(28) Li, C.; Li, L.; Sun, L.; Pei, Z.; Xie, J.; Zhang, S. Transformation of hydroquinone to benzoquinone mediated by reduced graphene oxide in aqueous solution. *Carbon* **2015**, *89*, 74−81.
(29) Xie, J.; Li, L.; Sun, L.; Pei, Z.; Wen, B.; Xing, B. Reduced graphene oxide-catalyzed oxidative coupling reaction of 4-methoxyphenol in aerobic aqueous solution. *Carbon* **2017**, *121*, 418−425.
(30) Terzyk, A. P. Further insights into the role of carbon surface functionalities in the mechanism of phenol adsorption. *J. Colloid Interface Sci.* **2003**, *268*, 301−329.
(31) Tessmer, C. H.; Vidic, R. D.; Uranowski, L. J. Impact of Oxygen-Containing Surface Functional Groups on Activated Carbon Adsorption of Phenols. *Environ. Sci. Technol.* **1997**, *31*, 1872−1878.
(32) Vidic, R. D.; Tessmer, C. H.; Uranowski, L. J. Impact of surface properties of activated carbons on oxidative coupling of phenolic compounds. *Carbon* **1997**, *35*, 1349−1359.
(33) Fang, G.; Gao, J.; Liu, C.; Dionysiou, D. D.; Wang, Y.; Zhou, D. Key role of persistent free radicals in hydrogen peroxide activation by biochar: implications to organic contaminant degradation. *Environ. Sci. Technol.* **2014**, *48*, 1902−1910.
(34) Luo, K.; Yang, Q.; Pang, Y.; Wang, D.; Li, X.; Lei, M.; Huang, Q. Unveiling the mechanism of biochar-activated hydrogen peroxide on the degradation of ciprofloxacin. *Chem. Eng. J.* **2019**, *374*, 520−530.
(35) Klüpfel, L.; Keiluweit, M.; Kleber, M.; Sander, M. Redox properties of plant biomass-derived black carbon (biochar). *Environ. Sci. Technol.* **2014**, *48*, 5601−5611.
(36) Xin, D.; Xian, M.; Chiu, P. C. New methods for assessing electron storage capacity and redox reversibility of biochar. *Chemosphere* **2019**, *215*, 827−834.
(37) Prévoteau, A.; Ronsse, F.; Cid, I.; Boeckx, P.; Rabaey, K. The electron donating capacity of biochar is dramatically underestimated. *Sci. Rep.* **2016**, *6*, No. 32870.
(38) Kappler, A.; Wuestner, M. L.; Ruecker, A.; Harter, J.; Halama, M.; Behrens, S. Biochar as an Electron Shuttle between Bacteria and Fe(III) Minerals. *Environ. Sci. Technol. Lett.* **2014**, *1*, 339−344.
(39) Saquing, J. M.; Yu, Y.-H.; Chiu, P. C. Wood-Derived Black Carbon (Biochar) as a Microbial Electron Donor and Acceptor. *Environ. Sci. Technol. Lett.* **2016**, *3*, 62−66.
(40) Yu, L.; Yuan, Y.; Tang, J.; Wang, Y.; Zhou, S. Biochar as an electron shuttle for reductive dechlorination of pentachlorophenol by Geobacter sulfurreducens. *Sci. Rep.* **2015**, *5*, No. 16221.
(41) Zhao, N.; Yin, Z.; Liu, F.; Zhang, M.; Lv, Y.; Hao, Z.; Pan, G.; Zhang, J. Environmentally persistent free radicals mediated removal of Cr(VI) from highly saline water by corn straw biochars. *Bioresour. Technol.* **2018**, *260*, 294−301.
(42) Cui, X.; Ni, Q.; Lin, Q.; Khan, K. Y.; Li, T.; Khan, M. B.; He, Z.; Yang, X. Simultaneous sorption and catalytic oxidation of trivalent antimony by Canna indica derived biochars. *Environ. Pollut.* **2017**, *229*, 394−402.
(43) Fang, G.; Liu, C.; Gao, J.; Dionysiou, D. D.; Zhou, D. Manipulation of persistent free radicals in biochar to activate persulfate for contaminant degradation. *Environ. Sci. Technol.* **2015**, *49*, 5645−5653.
(44) Liu, X.; Sen, S.; Liu, J.; Kulaots, I.; Geohegan, D.; Kane, A.; Puretzky, A. A.; Rouleau, C. M.; More, K. L.; Palmore, G. T. R.; Hurt, R. H. Antioxidant Deactivation on Graphenic Nanocarbon Surfaces. *Small* **2011**, *7*, 2775−2785.
(45) Zhong, D.; Jiang, Y.; Zhao, Z.; Wang, L.; Chen, J.; Ren, S.; Liu, Z.; Zhang, Y.; Tsang, D. C. W.; Crittenden, J. C. pH Dependence of Arsenic Oxidation by Rice-Husk-Derived Biochar: Roles of Redox-Active Moieties. *Environ. Sci. Technol.* **2019**, *53*, 9034−9044.
(46) Qin, W.; Wang, Y.; Fang, G.; Wu, T.; Liu, C.; Zhou, D. Evidence for the generation of reactive oxygen species from hydroquinone and benzoquinone: Roles in arsenite oxidation. *Chemosphere* **2016**, *150*, 71−78.
(47) Zhang, K.; Sun, P.; Faye, M. C. A. S.; Zhang, Y. Characterization of biochar derived from rice husks and its potential in chlorobenzene degradation. *Carbon* **2018**, *130*, 730−740.
(48) Parra, S.; Olivero, J.; Pacheco, L.; Pulgarin, C. Structural properties and photoreactivity relationships of substituted phenols in TiO_2 suspensions. *Appl. Catal., B* **2003**, *43*, 293−301.
(49) Torres, R. A.; Torres, W.; Peringer, P.; Pulgarin, C. Electrochemical degradation of p-substituted phenols of industrial interest on Pt electrodes. Attempt of a structure−reactivity relationship assessment. *Chemosphere* **2003**, *50*, 97−104.
(50) Franz, M.; Arafat, H. A.; Pinto, N. G. Effect of chemical surface heterogeneity on the adsorption mechanism of dissolved aromatics on activated carbon. *Carbon* **2000**, *38*, 1807−1819.
(51) Li, L.; Quinlivan, P. A.; Knappe, D. R. U. Effects of activated carbon surface chemistry and pore structure on the adsorption of organic contaminants from aqueous solution. *Carbon* **2002**, *40*, 2085−2100.
(52) Pendleton, P.; Wong, S. H.; Schumann, R.; Levay, G.; Denoyel, R.; Rouquero, J. Properties of activated carbon controlling 2-Methylisoborneol adsorption. *Carbon* **1997**, *35*, 1141−1149.
(53) MacDonald, J. A. F.; Evans, M. J. B. Adsorption and enthalpy of phenol on BPL carbon. *Carbon* **2002**, *40*, 703−707.
(54) Müller, E. A.; Rull, L. F.; Vega, L. F.; Gubbins, K. E. Adsorption of Water on Activated Carbons: A Molecular Simulation Study. *J. Phys. Chem. A* **1996**, *100*, 1189−1196.
(55) Müller, E. A.; Hung, F. R.; Gubbins, K. E. Adsorption of water vapor− methane mixtures on activated carbons. *Langmuir* **2000**, *16*, 5418−5424.
(56) Wang, Y.; Ao, Z.; Sun, H.; Duan, X.; Wang, S. Activation of peroxymonosulfate by carbonaceous oxygen groups: experimental and density functional theory calculations. *Appl. Catal., B* **2016**, *198*, 295−302.
(57) Menumerov, E.; Hughes, R. A.; Neretina, S. Catalytic Reduction of 4-Nitrophenol: A Quantitative Assessment of the Role of Dissolved Oxygen in Determining the Induction Time. *Nano. Lett.* **2016**, *16*, 7791−7797.
(58) Tang, J.; Tang, L.; Feng, H.; Zeng, G.; Dong, H.; Zhang, C.; Huang, B.; Deng, Y.; Wang, J.; Zhou, Y. pH-dependent degradation of p-nitrophenol by sulfidated nanoscale zerovalent iron under aerobic or anoxic conditions. *J. Hazard. Mater.* **2016**, *320*, 581−590.
(59) Peng, X.; Liu, X.; Zhou, Y.; Peng, B.; Tang, L.; Luo, L.; Yao, B.; Deng, Y.; Tang, J.; Zeng, G. New insights into the activity of a biochar supported nanoscale zerovalent iron composite and nanoscale zero valent iron under anaerobic or aerobic conditions. *RSC Adv.* **2017**, *7*, 8755−8761.
(60) Geeta, S.; Sharma, S. B.; Rao, B. S. M.; Mohan, H.; Dhanya, S.; Mittal, J. P. Study of kinetics and absorption spectra of OH adducts of hydroxy derivatives of benzaldehyde and acetophenone. *J. Photochem. Photobiol., A* **2001**, *140*, 99−107.
(61) Buxton, G. V.; Greenstock, C. L.; Helman, W. P.; Ross, A. B. Critical review of rate constants for reactions of hydrated electrons, hydrogen atoms and hydroxyl radicals ($^{\cdot}OH/^{\cdot}O^-$) in aqueous solution. *J. Phys. Chem. Ref. Data* **1988**, *17*, 513−886.

https://dx.doi.org/10.1021/acs.est.0c04991
Environ. Sci. Technol. XXXX, XXX, XXX−XXX

(62) Grant, T. M.; King, C. J. Mechanism of irreversible adsorption of phenolic compounds by activated carbons. *Ind. Eng. Chem. Res.* **1990**, *29*, 264−271.
(63) Ma, Z.; Sun, Q.; Ye, J.; Yao, Q.; Zhao, C. Study on the thermal degradation behaviors and kinetics of alkali lignin for production of phenolic-rich bio-oil using TGA−FTIR and Py−GC/MS. *J. Anal. Appl. Pyrolysis* **2016**, *117*, 116−124.
(64) Huang, Q. G.; Weber, W. J. Transformation and Removal of Bisphenol A from Aqueous Phase via Peroxidase-Mediated Oxidative Coupling Reactions:Efficacy,Products,and Pathways. *Environ. Sci. Technol.* **2005**, *39*, 6029−6036.
(65) Lu, J.; Shao, J.; Liu, H.; Wang, Z.; Huang, Q. Formation of Halogenated Polyaromatic Compounds by Laccase Catalyzed Transformation of Halophenols. *Environ. Sci. Technol.* **2015**, *49*, 8550−8557.

https://dx.doi.org/10.1021/acs.est.0c04991
Environ. Sci. Technol. XXXX, XXX, XXX−XXX